ARCHIVES OF MECHANICAL TECHNOLOGY AND MATERIALS

Microstructure, phase composition and corrosion resistance of Ni_2O_3 coatings produced using laser alloying method

Aneta Bartkowska[a*], Damian Przestacki[a], Tadeusz Chwalczuk[a]

[a]*Poznan University of Technology, Piotrowo 3 Street, 60-965 Poznan, Poland*

e-mail address: aneta.bartkowska@put.poznan.pl

A B S T R A C T

The paper presents the studies' results of microstructure, microhardness, cohesion, phase composition and the corrosion resistance analysis of C45 steel after laser alloying with nickel oxide (Ni_2O_3). The aim of the laser alloying was to obtain the surface layer with new properties through covering C45 steel by precoat containing modifying compound, and then remelting this precoat using laser beam. As a result of this process the surface layer consisting of remelted zone and heat affected zone was obtained. In the remelted zone an increased amount of modifying elements was observed. It was also found that the surface layer formed during the laser alloying with Ni_2O_3 was characterized by good corrosion resistance. This property has changed depending on the thickness of the applied precoat. It was observed that the thickness increase of nickel oxides precoat improves corrosion resistance of produced coatings.

Key words: laser alloying; Ni_2O_3 oxide; microstructure; microhardness; corrosion resistance

1. INTRODUCTION

Surface technologies such as laser heat treatment by using elements (e.g. B, C, N, Si, Cr, Ni, Mo) [1-7], intermetallic phases [8] or ceramic powders [7, 9] enable shaping characteristics of materials, giving them new properties, including increased durability and reliability as well as corrosion resistance. The modification of surface layers has been discussed in numerous publications. The authors modify the layer by using the laser beam [1-7, 9-11] as well as using the plasma jet [8, 12].

The influence of a laser beam on the modification of a surface layer containing elements such as Cr [2], Si [3], C [4], N [5], Ni [6], Mo [7], has been analyzed by researchers in mentioned papers. Lasers are widely used in surface engineering. Adequate selection of alloy additives and process parameters allows to obtain surface layers with new properties [1-9, 11, 13]. Often, these properties are impossible to obtain with traditional methods of surface treatment. Rapid heating and subsequent rapid cooling of the material lead to the obtaining of the fine crystalline microstructure, highly supersaturated with the selected element [13]. Surface and heat treatment using a laser beam is advantageous because it results in beneficial microhardness, high wear resistance and good corrosion resistance [1-7, 9-11, 13]. The appropriate selection of the surface material and the treatment parameters lead to the extension of the life cycle of the product [1-12] In the paper [7] authors presented analysis of corrosion and wear resistance of NiTi surface after the modification by Mo and ZrO_2 using a laser beam. The modified layers were free from microcracks and porosity. ZrO_2 and Mo were successfully used to the surface alloying of NiTi alloy by laser technology. The microhardness values of Mo and ZrO_2 alloyed layers were improved to 660 HV and 720 HV respectively, from value 220 HV corresponding microhardness of NiTi substrate. The increase of the microhardness accompanied the increase of the wear resistance. The produced surface layers improved wear resistance about six times in comparison with NiTi without modified layers [7].

In the paper presented by Labisz et al. [9] the authors focused on the investigation of mechanical properties and microstructure of the hot-work tool steel after laser modification by using powders of aluminium and zirconium oxides. After the laser modification using selected oxides the microstructure of the specimens was changed. The authors revealed the presence of remelting zone and heat affected zone. In this second zone, the grains were larger and not so homogeneous as in the metal matrix. The laser alloying of hot-work tool steels seems to be very attractive for automotive and other heavy industries.

This paper focuses on problems of corrosion resistance of steel after laser alloying with nickel oxides. The influence of different thickness of the Ni_2O_3 coating on microstructure,

microhardness, phase composition and corrosion resistance were studied and compared.

2. EXPERIMENTAL PROCEDURE

The aim of the study was to evaluate the impact of laser alloying with nickel oxide (Ni_2O_3) on the basis of changes in microstructure, microhardness profiles, corrosion resistance and cohesion. The tests were carried out on C45 steel which chemical composition is given in Table 1 (according to PN-EN 10083-2:2008).The samples of 60 mm length, 12 mm width and 4 mm height were used for this study. The study results of the laser alloying Ni_2O_3 oxide of C45 steel were compared with the laser remelting of C45 steel without a precoat. The Ni_2O_3 coating was applied in paste form, which consisted of Ni_2O_3 oxide, water glass and distilled water.

The thicknesses of Ni_2O_3 oxide coating were 50 µmand 200 µm. The coating thicknesses were determined based on the average of 10 measurements on a sample by means of ultrameter A2002M and were in the range of +/−5 µm.

Table 1. Chemical composition of C45 steel [wt.%]

C	Mn	Si	P	S	Cr	Ni	Mo
0.42	0.72	0.19	0.008	0.03	0.2	0.12	0.08

The laser alloying was carried out using TruDiode 3006 diode laser of nominal power equal to3.0 kW. The parameters used in the experiment were as follows: laser beam power (P) – 0.3 kW, 0.6 kW, 0.9 kW; scanning laser beam velocity (v_l) – 48 mm/s. Laser tracks were arranged as multiple tracks with a distance f = 0.5 mm, where f was the distance between axes of adjacent tracks. Overlap of laser tracks was equal to 50%. Laser head of TrumpfTruDiode 3006 is maintained on KUKA KR16-2 robot. The scheme of laser heat treatment process was presented in Figure 1. Laser TEM_{00} and laser beam diameter was d_l=1mm.

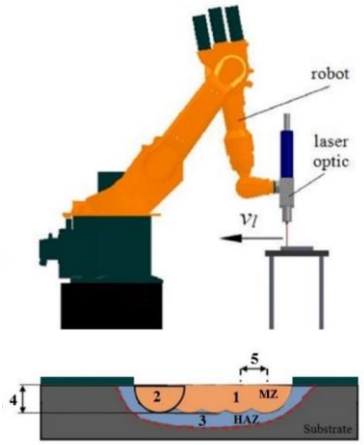

Fig. 1. Scheme of laser heat treatment process; designations: 1 – processed coating, 2 – heating area by laser beam, 3 – heat affected zone, 4 – depth of melted pool, 5 – overlap

Prior to the laser heat treatment (LHT) the specimens were hardened in water from 850 °C and tempered at 570 °C for 1h. The scheme of layers production using the laser alloying Ni_2O_3 oxide paste method is presented in Figure 2. The process of production of layers was composed of the heat treatment initial pearlite-ferrite substrate (Step 1), followed by Ni_2O_3 oxide paste application (Step 2) and completed with the laser modification of steel with Ni_2O_3 oxide paste (Step 3). As a result of the laser beam action on the cover and the substrate a new layer was obtained consisting of three zones: remelted (MZ), heat affected (HAZ) and substrate.

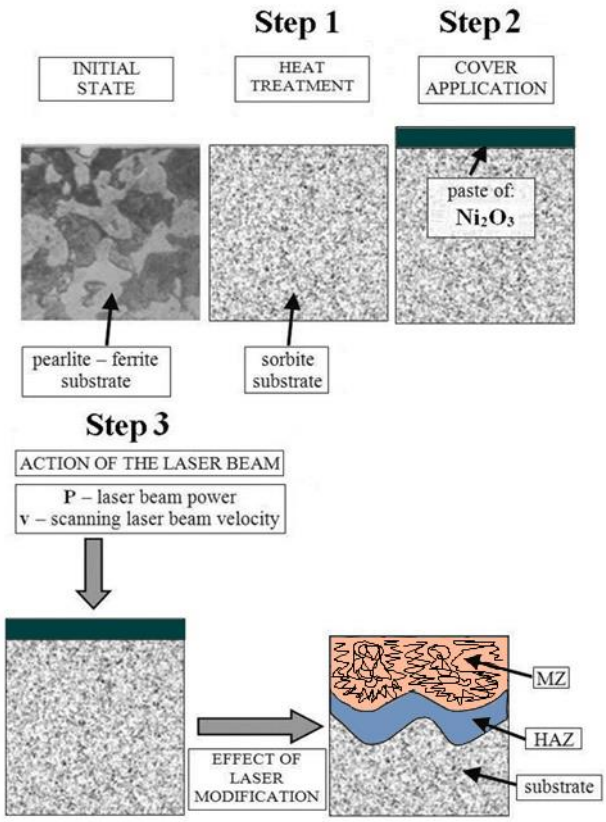

Fig. 2. Scheme of laser alloying with Ni_2O_3 oxide

Microstructure studies were performed using a light microscope Metavalfrom Carl Zeiss Jena with a digital camera 2300 3.0 MP and Live Motic Images Plus 2.0 Resolution software. Metallographic observations of the microstructure were conducted on polished and etched cross-sections of the samples in a 2% solution of HNO_3 and Marble's reagent. The phase analysis of the nickel oxide layer was performed on EMPYREAN PANalytical X-Ray diffractometer using Cu Kα radiation.

To determine microhardness profiles a ZWICK 3212 B Vickers hardness tester was used with indentation load of 100 G (HV0.1). Corrosion resistance of laser modified layers was carried out in a 5 % solution of NaCl at a temperature of 22°C on the surface of 50 mm^2. The studies were performed on a potentiostat-galvanostat ATLAS 0531 EU & IA ATLAS SOLLICH. Auxiliary electrode was a platinum electrode, and the reference electrode was a saturated calomel electrode. The test procedure and recording of the results were performed using AtlasCorr and AtlasLab software. The

polarization of the samples was carried out in the direction of the anode in the range of potentials from -1.4 V to +0.6 V. The study was conducted at a rate of change in potential of 0.5 mV/sec. Based on the analysis of current curves potentiodynamic corrosion and corrosion potential were determined. Adhesion tests of surface layers were conducted in accordance with the standard VDI 3198 [14]. This method consisted of comparing Rockwell indentations with scale standards as presented in Figure 3.

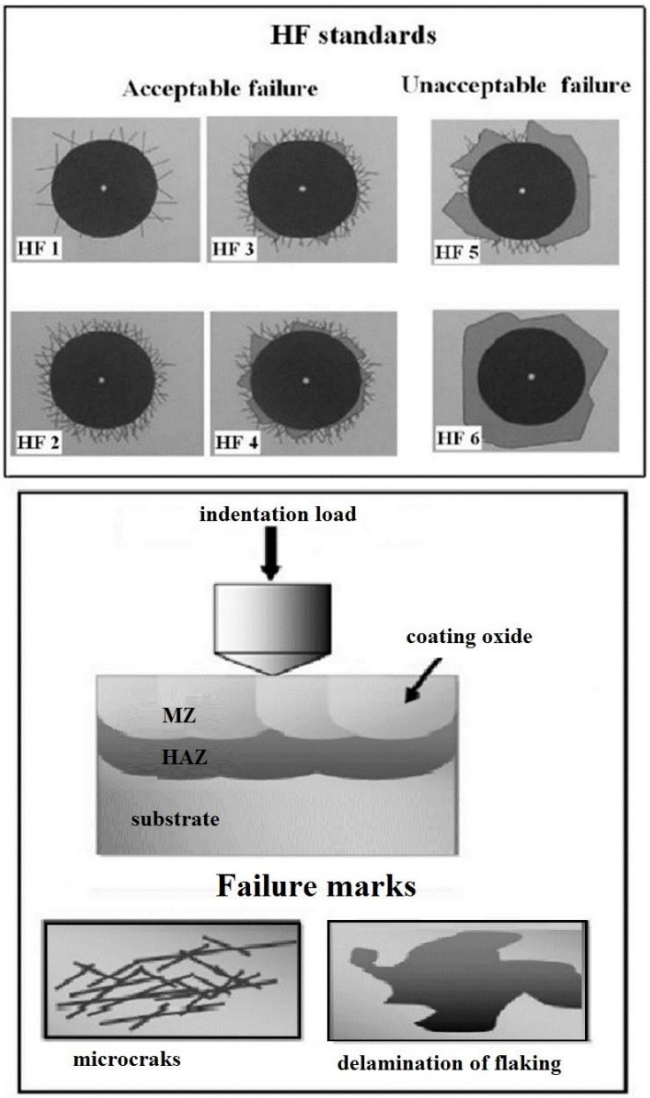

Fig. 3. Scale of models to test cohesion

A standard Rockwell tester as a destructive quality test for examined layers was employed in this study and damage to the layers was compared to the adhesion strength quality maps HF1-HF6 (Fig. 3). In general, the adhesion strength quality HF1-HF4 defined acceptable failure, whereas HF5 and HF6 represented unacceptable failure [14]. Hardness test was performed on Rockwell 610A hardness tester.

3. RESULTS

Ni_2O_3 powder morphology is shown in Figure 4. The Ni_2O_3 powder particles were of spherical shape with the size in the range of 10 – 20 μm.

The microstructure after the laser alloying with Ni_2O_3 oxide is shown in Figures 5 and 6; and after the laser remelting C45 steel in Figure 7. The microstructure after the laser modification (laser alloying or laser remelting) consisted of three zones: remelted zone (MZ), heat affected zone (HAZ) and substrate (Figs. 5a, 6a). The microstructure of nickel oxide enriched remelted zone contained supersaturated solid Ni_2O_3 solution with martensite. Heat affected zone was composed of martensite needles, and the substrate with sorbite structure.

As a result of remelting of the layers, laser track microstructure was composed of both surface layers' materials (Ni_2O_3) and substrate material. Fluctuations in the melting pool in new layers are clearly visible in Figure 6a.

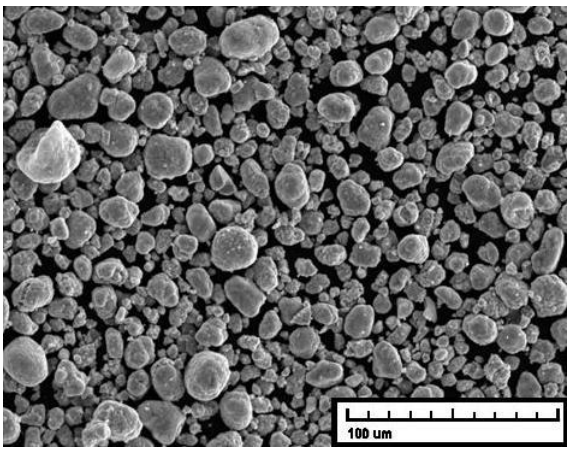

Fig.4. Ni_2O_3 powder morphology

The remelted laser tracks had a thickness of approximately 500 μm (Fig. 7a), whereas the alloyed laser tracks had a thickness of approximately 500 - 600 μm (Figs. 5a, 6a). The thickness of alloyed laser tracks was related to the thickness of the oxide coating (50 μm –Fig. 5a; 200 μm – Fig. 6a). In both cases the thickness in the area of the remelted zone on the border tracks was lower than at the axes of the tracks. The tracks after the laser alloying had a deeper remelted zone than the tracks after the laser remelting. The depth of the remelted zone after the laser remelting and the laser alloying were similar and had a thickness of approximately 200 μm (Figs. 5a – 7a).

The results of metallographic study revealed that the microstructure of solidifying material after the laser alloying with nickel oxide was characterized by the appearance of the areas of varied morphology. These areas were established as a result of the crystallization of the newly-formed surface layer. Multiple changes in the direction of crystal formation were observed in these areas. In the border region between solid and liquid phases fine dendrites were present. Their main axes were parallel to the heat conduction direction.

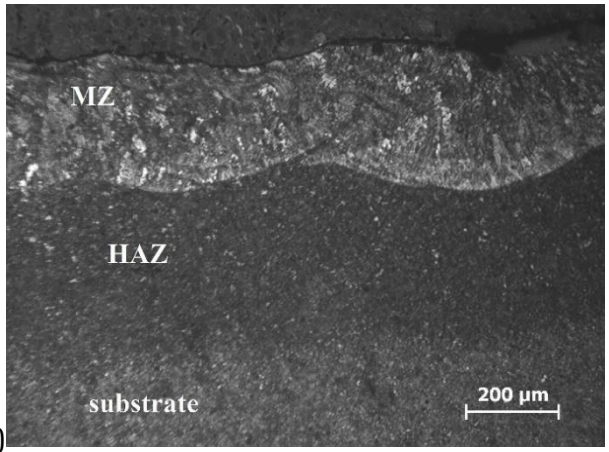

a)

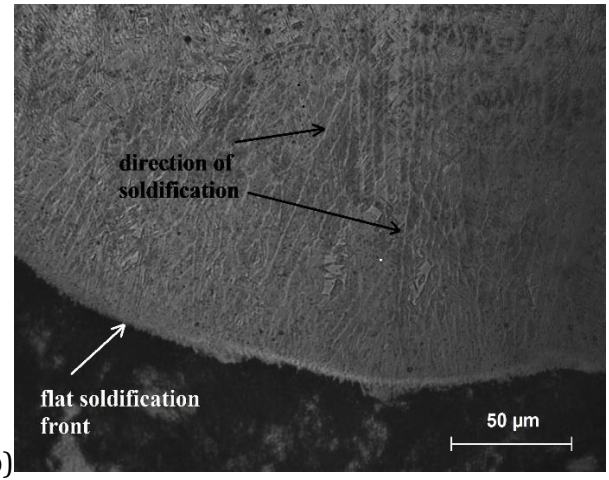

b)

Fig. 5. Microstructure of laser alloying with Ni_2O_3 oxide layerLHT: Ni_2O_3paste - 50µm, P = 0.6 kW, v_l = 48 mm/s, f = 0.50 mm; a) laser tracks after eatching with 2% solution of HNO_3, b) remelted zone after eatching with Marble's reagent

Significantly smaller size crystals in the lower area of the remelted zone in comparison with the central area is related to the initiation of solidification process on undissolved phases of the remelted material. In the subsequent stage of the solidification process the direction of the crystal formation is closely connected with the preservation of privileged orientation, or it is identical to the direction of the highest temperature gradient (Figs. 5b, 6b, 7b).

As a result of the laser alloying a microstructure which was free from defect with district refinement of the substrate, enriched with the alloying phase. Within the microstructure of the laser track a flat solidification front at the border of the remelted zone and heat affected zone was observed (Fig. 5b). The flat solidification front transformed into column and dendritic crystals in the direction of carried away heat (Fig. 7b).

The intensive mixing of substrate material and alloying compound (Ni_2O_3) takes places in the liquid pool due to convection or gravity movements as well as due to the laser beam pressure. After the laser alloying with Ni_2O_3 nickel oxide and iron oxide phases were identified in the layer.

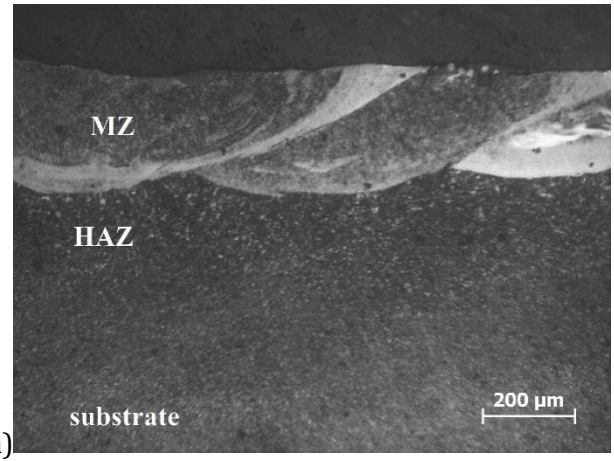

a)

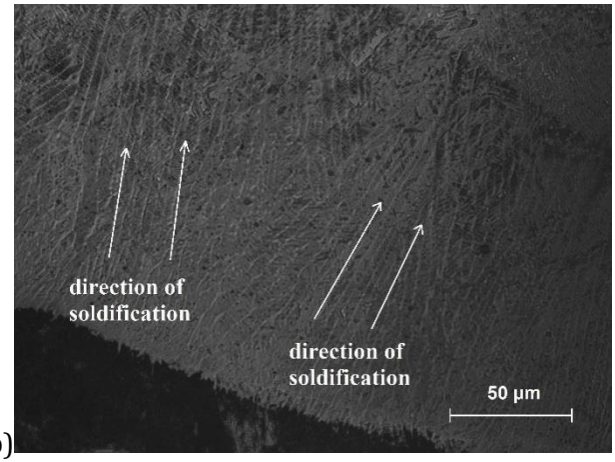

b)

Fig. 6. Microstructure of laser alloying with Ni_2O_3 oxide layerLHT: Ni_2O_3paste - 200µm, P = 0.6 kW, v_l = 48 mm/s,f = 0.50 mm: a) laser tracks after eatching with 2% solution of HNO_3, b) remelted zone after eatching with Marble's reagent

The peak intensity in the laser alloyed with Ni_2O_3 oxides layers increases with the increase of the coating thickness (Fig. 8). Microhardness profiles on the cross-section of the treated layers as a function of the distance from the surface in the samples studied were presented in Figures 9-11.

The microhardness was tested along the axes and along the interface of the laser tracks. The microhardness in the remelted zone of the laser alloying with Ni_2O_3 oxides layer was about 400 – 600 HV 0.1 (Figs. 9, 10). The microhardness is similar in the axes and at the interface of the laser tracks, in the remelted zone. The diameter of the tracks is dependent on aggregated impacts of the laser beam and laser tracks distribution. In all layers the microhardness in heat affected zone reached 400 HV0.1 and decreased towards the substrate - 320 HV0.1.

The difference in microhardness on the cross-section of the remelted zone of a track laser alloyed with nickel oxide of 200 µm was caused by multiple fluctuations of the chemical composition in the laser treated zone.

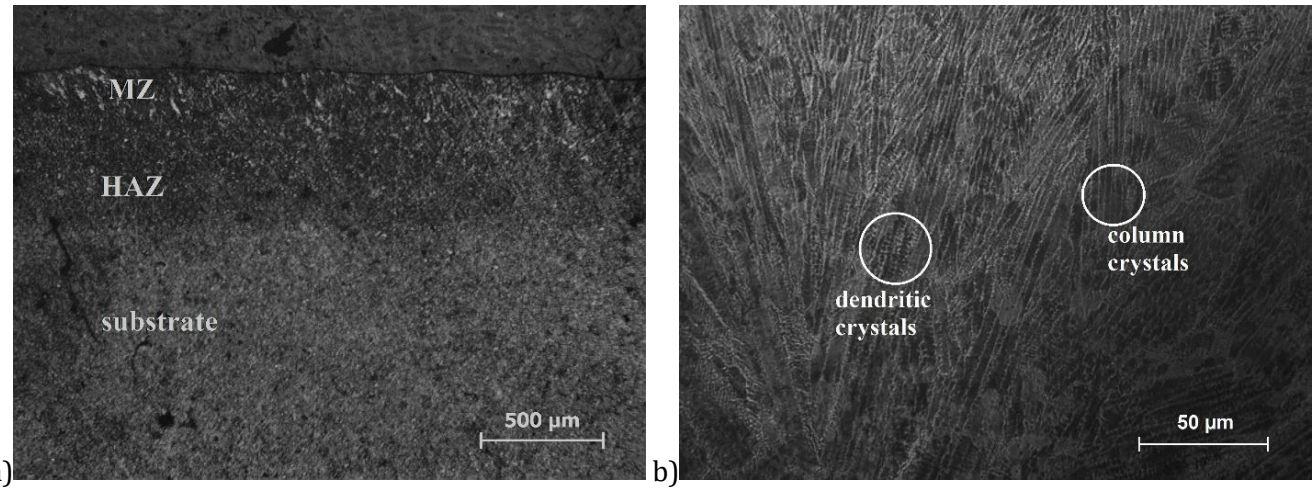

Fig. 7. Microstructure of laser remelting of C45 steelLHT: P = 0.6 kW, v_l = 48 mm/s, f = 0.50 mm: a) laser tracks after eatching with 2% solution of HNO_3, b) remelted zone after eatching with Marble's reagent

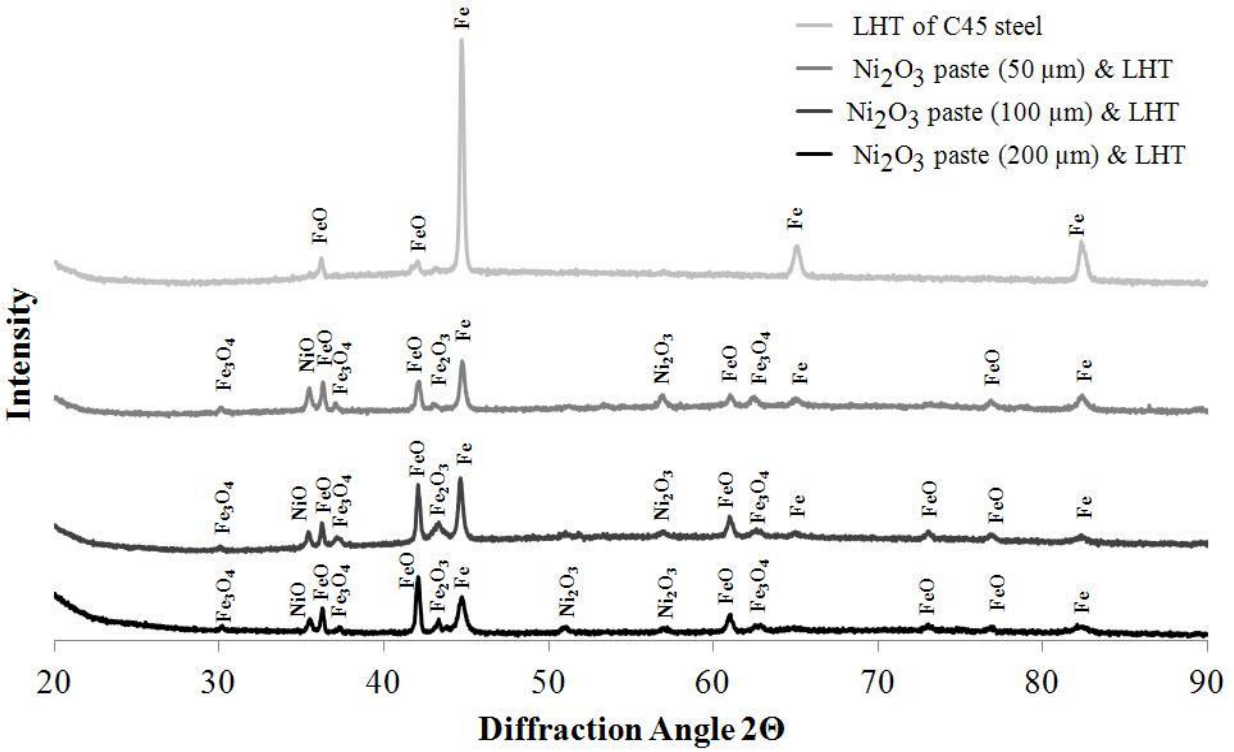

Fig.8. X-ray diffraction pattern of Ni_2O_3 oxide layer after LHT

The results of corrosion tests were shown in Figure 12. It shows the current density curves as a function of predetermined potential, where the values of electrochemical parameters were determined based on the analysis of the curves. The values of electrochemical parameters were shown in Table 2. A layer after a laser alloyed with nickel oxide of 50 µm is characterized by corrosion resistance in comparison to the laser remelted steel. This is probably due to the fact that the alloying layer was too thin. Remelting the oxide layer with a laser beam P = 0.6 kW produced a layer four times thicker. Increasing the depth of the remelted area resulted in oxide layer dissolving in the steel substrate, thus decrease corrosion resistance. The microhardness comparable with laser alloyed steel also proves that the alloying layer was too thin. Application of a thicker oxide layer (200µm) with the same laser heat treatment parameters increased not only microhardness but also corrosion resistance.

Figure 13 shows the results of the study of surface cohesion of the layers. In each case analyzed, surface layers are formed on a scale of acceptable failures based on VDI standard 3198 (Fig. 3). Figure 13 shows an image of Rockwell indentation on the surface of a laser alloyed with Ni_2O_3 steel.

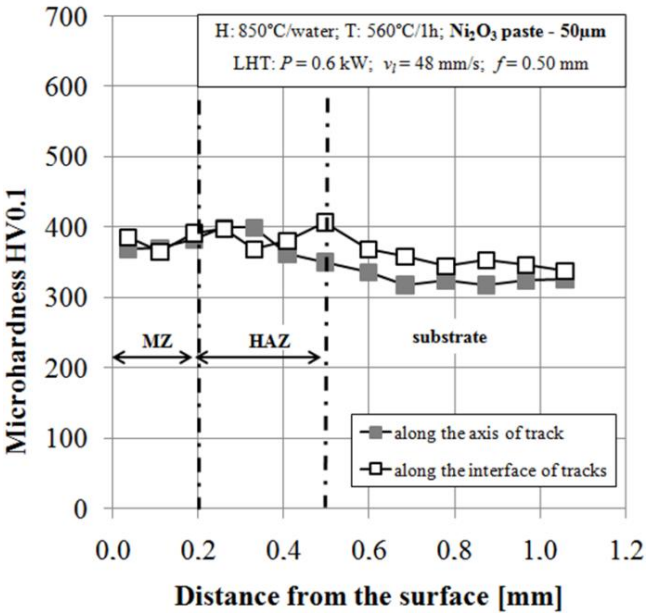

Fig. 9. Microhardness profiles of laser alloying with Ni_2O_3 oxide layer; LHT: Ni_2O_3paste – 50µm, P = 0.6 kW, v_l = 48 mm/s, f = 0.50 mm

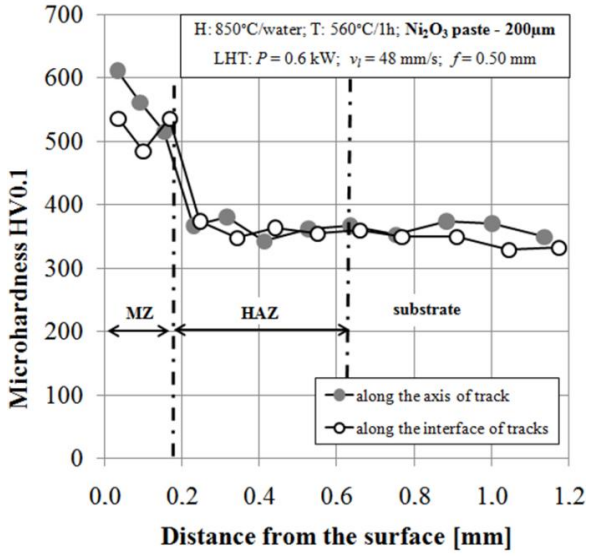

Fig. 10. Microhardness profiles of laser alloying with Ni_2O_3 oxide layer; LHT: Ni_2O_3paste – 200µm, P = 0.6 kW, v_l = 48 mm/s, f = 0.50 mm

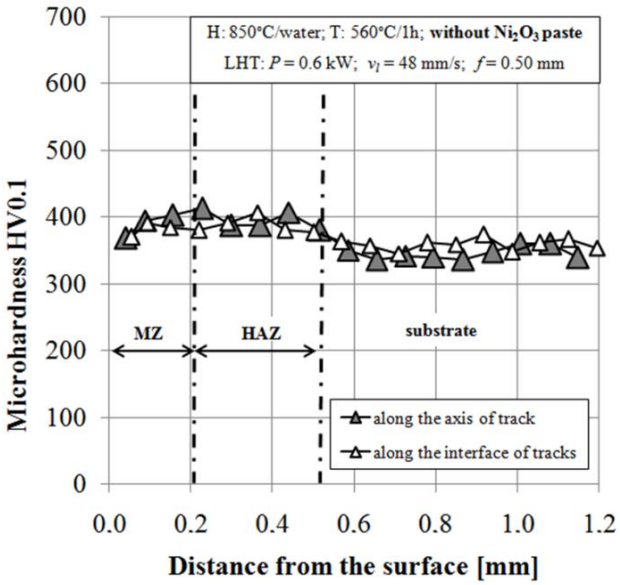

Fig. 11. Microhardness profiles of laser remelting of C45 steel; LHT: P = 0.6 kW, v_l = 48 mm/s, f = 0.50 mm

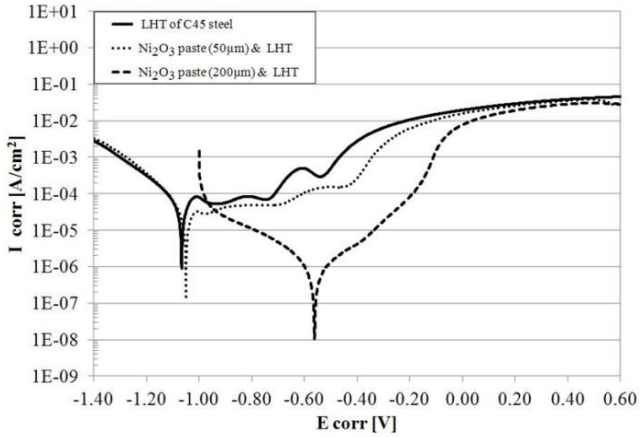

Fig. 12. Corrosion resistance of C45 steel after laser remelting and laser alloying with Ni_2O_3 oxide in NaCl solution - E corr: -1.40 ÷ -0.60 V

It can be seen that there are no cracks on the layer and the edge surrounding the indentation is smooth. Adhesion of the surface layer with Ni_2O_3 is good and it conforms to the standard in terms of HF1. Such good cohesion of the surface layer formed by its remelting with the substrate can also result from the fact that the new layer has microhardness in the range of 600 – 500HV0.1. Varying power of the laser beam applied in this study along with a constant scanning beam velocity were optimal for P = 0.6 kW. At low laser beam power P = 0.3 kW the layer was not remelted and did not permanently bond with the substrate. Too high laser beam power, however, (P = 0.9 kW) slowed down the solidification, thus reducing microhardness as compared to hardened and tempered substrate.

Table 2.Corrosion current and corrosion potential of C45 steel samples after laser heat treatment

Sample	Corrosion current I_{corr} [A·cm^2]	Corrosion potential E_{corr} [V]
LHT of C45 steel	7.25 E-06	-1.07 E+00
Ni_2O_3 paste (50 µm) & LHT of C45 steel	6.25 E-06	-1.05 E+00
Ni_2O_3 paste (200 µm) & LHT of C45 steel	2.16 E-07	-5.62 E-01

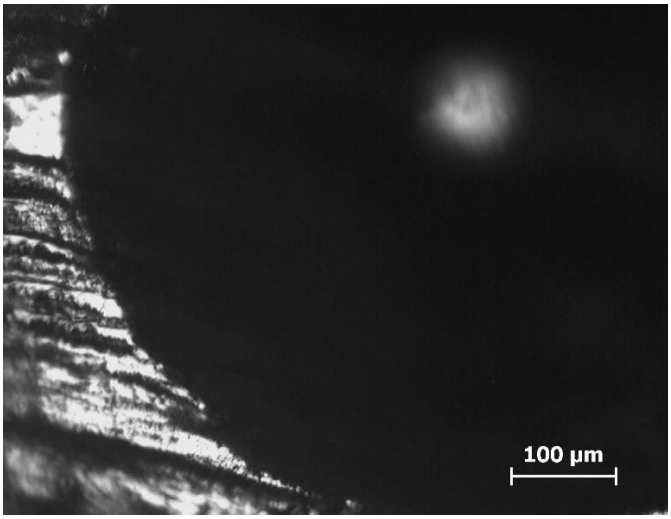

Fig. 13. Rockwell indentation image made on C45 steel after laser alloying with Ni_2O_3 oxide

4. CONCLUSIONS

- The microstructure of surface layers after laser alloying with nickel oxides is composed of three zones: remelted, heat affected and substrate. Between the remelted zone and the heat affected zone, the flat solidification front was visible, which transformed into column and dendritic crystals.
- Microhardness measurements revealed a mild gradient of microhardness from remelted zone (600 -400 HV0.1) into the substrate material (approx. 300 HV0.1). It was found that the layers had a good cohesion with the substrate.
- As a result of laser modification process using nickel oxides the corrosion resistance was increased. It can be concluded that the increased thickness of nickel oxides precoat improves corrosion resistance.

ACKNOWLEDGMENTS

The authors wish to thank dr. A. Miklaszewski for his help in performing of XRD studies.

This work has been financially supported by Ministry of Science and Higher Education in Poland as a part of the 02/24/DSPB project.

REFERENCES

[1] Morimoto J., Ozaki T., Kubohori T., Morimoto S., Abe N., Tsukamoto M., Some properties of boronized layers on steels with direct diode laser. Vacuum, 83(2009) 185-189.
[2] Woldan A., Kusiński J., Kąc S., Laser surface alloying of plain carbon steel with chromium powder. Materials Engineering POLAND, 140 (2004) 689-692.
[3] Bartkowska A., Pertek-Owsianna A., Bartkowski D., Popławski M., Przestacki D., Wear and corrosion resistance of C45 steel laser alloyed with boron and silicon. Journal of Research and Applications in Agricultural Engineering, 59 (2014) 10-14.
[4] Katsamas A. I., Haidemenopoulos G. N., Laser-beam carburizing of low-alloy steels. Surface and Coatings Technology, 139 (2001) 183-191.
[5] Bartkowska A., Pertek A., Laser surface modification of nitrided 42CrMo4 steel. Conference materials: II International Interdisciplinary Technical Conference of Young Scientists, INTERTECH 2009, Poznan, Poland, (2009) 43-45.
[6] Bartkowska A., Pertek A., Laser production of B-Ni complex layers. Surface & Coatings Technology, 248 (2014) 23-29.
[7] Ng K.W., Man H.C., Yue T.M., Corrosion and wear properties of laser surface modified NiTi with Mo and ZrO_2. Applied Surface Science 254 (2008) 6725–6730.
[8] Miklaszewski A., Jurczyk M.U., Jurczyk M., Surface Modification of Pure Titanium by TiB Precipitation. Solid State Phenomena, 183 (2012) 131-136.
[9] Labisz K., Dobrzański L.A., Jonda E., Lelątko J., Comparison of surface laser alloying of chosen tool steel using Al_2O_3 and ZrO_2 powder. Journal of Achievements in Materials and Manufacturing Engineering, 39 (2010) 87-94.
[10] Wang A.H., Wang W.Y., Xie C.S., Song W.L., Zeng D.W., Hu J. H., CO_2 laser-induced structure changes on an alumina–mullite–zirconia refractory. Applied Surface Science 233 (2004) 244-251.
[11] Przestacki D., Conventional and laser assisted machining of composite A359/20SiCp. Procedia CIRP, 14 (2014) 229-233.
[12] Chicota D., Duarte G., Tricoteaux A., Jorgowski B., Leriche A., Lesage J., Vickers Indentation Fracture (VIF) modeling to analyze multi-cracking toughness of titania, alumina and zirconia plasma sprayed coatings. Materials Science and Engineering A, 527 (2009) 65-76.
[13] Steen W.M., Laser material processing-an overview. Journal of Optics A: Pure and Applied Optics 5 (2003) S3-S7.
[14] VereinDeutscherIngenieureNormen, VDI 3198, 1991.